Magnetic properties of the flux line lattice in paramagnetic superconductors

1997 J. Phys.: Condens. Matter 9 2239

(http://iopscience.iop.org/0953-8984/9/10/012)

J. Phys.: Condens. Matter **9** (1997) 2239–2258. Printed in the UK PII: S0953-8984(97)78271-7

Magnetic properties of the flux line lattice in paramagnetic superconductors

Damian P Hampshire

Superconductivity Group, Department of Physics, University of Durham, South Road, Durham DH1 3LE, UK

Received 20 December 1996

Abstract. In this work, superconductors that contain paramagnetic ions which only interact with the superelectrons via electromagnetic fields are considered. We postulate that when these materials are superconducting, a consequence of the phase coherence of the superelectrons is that if the external field is changed, after equilibrium is reached, there is no net heat produced or absorbed by the paramagnetic ions. We find that in high magnetic fields, when the susceptibility (χ) of the paramagnetic ions is such that $0 \leqslant \chi \ll 1$, the superconductor behaves like a standard type II material and for $\chi \gg 1$, the material behaves ferromagnetically such that there is a square flux line lattice. The magnetic phases present for different values of χ and magnetic field are described, and experimental evidence for them is provided.

1. Introduction

The coexistence of magnetism and superconductivity in the rare-earth Chevrel phases (RE)Mo_6S_8 and (RE)Mo_6Se_8, the ternary rhodium borides (RE)Rh_4B_4 and more recently the high-temperature superconductors where the crystal structure separates the superconducting electrons from the rare-earth 4f electrons which cause the magnetism has been the subject of intense study [1, 2]. These materials have provided many complex phase diagrams showing re-entrant superconductivity, field-induced superconductivity, the coexistence of superconductivity and magnetism at the atomic level and more recently, using neutron scattering, the existence of a square flux line lattice in high fields [3].

In this work, a subset of magnetic superconductors, described here as paramagnetic superconductors, is considered. In the normal state these materials are paramagnetic, but when they are superconducting, the electrons responsible for the paramagnetism are completely separated from the superelectrons so they only interact via magnetic fields. Therefore there is no pair-breaking mechanism which causes competition between superconductivity and magnetism [4].

We postulate that in the superconducting state, a consequence of the phase coherence of the superelectrons is that if the external field is changed, there is no net heat produced or absorbed by the paramagnetic ions. This is in contrast to the situation for the normal state; if the external field is increased, the temperature of the material increases. If the external field is decreased, the material cools (for example during adiabatic demagnetization). It is shown that much of the complexity of the magnetic phase diagrams of many magnetic superconductors can be explained in a self-consistent description without the need to introduce parameters unrelated to the superconductivity.

0953-8984/97/102239+20$19.50

In the next six sections, expressions for the magnetic properties are derived. Section 2 considers the Ginzburg–Landau equations for non-magnetic superconductors and how to extend them for paramagnetic superconductors. Section 3 considers how the paramagnetic ions reach thermal equilibrium after the external magnetic field has been changed. Sections 4, 5 and 6 provide calculations of the high-field and low-field properties of paramagnetic superconductors. In section 7, the structure of the flux line lattice is considered—in particular, whether the structure is triangular or square. The final three sections provide a comparison between the calculations and results found in the literature.

2. The Ginzburg–Landau equations

2.1. Non-magnetic superconductors

One of the most productive frameworks for describing the properties of superconductors in magnetic fields is through the Ginzburg–Landau [5, 6] formulism. Although only strictly applicable close to the critical temperature, it is useful for type II superconductors throughout their superconducting phase.

The Landau free energy is a minimum for the equilibrium stable superconducting phase and is given by

$$F_s(H,T) = F_n(0,T) + \alpha|\psi|^2 + \frac{1}{2}\beta|\psi|^4 + \frac{1}{2m}|(-\mathrm{i}\hbar\boldsymbol{\nabla} - 2e\boldsymbol{A})\psi|^2 + \frac{B^2}{2\mu_0} \tag{1}$$

where $F_s(H,T)$ is the free energy per unit volume in the superconducting phase at an applied field H and temperature T, $F_n(0,T)$ is the free energy per unit volume in the normal phase in zero field as a function of temperature, ψ is the wavefunction for the superconductor, α and β are constants, $\mu_0 H$ is the applied field, $\boldsymbol{B}$ is the total local magnetic field and $\boldsymbol{A}$ is the total local magnetic vector potential. The expression is phenomenological and can be justified as follows: the second and third terms, involving α and β, account for the reduction in energy when the normal electrons condense and become superelectrons; the fourth term accounts for the kinetic energy of the superelectrons in a magnetic field; and the last term known as the magnetic field energy accounts for the energy stored in the local magnetic fields.

2.2. The magnetic field energy for magnetic superconductors

The magnetic field energy term in a non-magnetic superconductor

$$\frac{B^2}{2\mu_0}$$

can be justified [6] by considering the energy per unit volume required to produce a field in a coil. We suggest that the magnetic field energy term be changed for paramagnetic superconductors as follows: the energy per unit volume (U_1) required to energize a coil in a paramagnetic medium is given by

$$U_1 = \frac{B^2}{2\mu_0(1+\chi)}$$

where $\boldsymbol{B}$ is the total field inside the coil and χ is the susceptibility of the paramagnetic medium.

In normal paramagnetic materials, as the field is increased, there is a redistribution of the magnetic moments parallel and antiparallel to the applied field as the ions thermally equilibrate. This generates heat ($U_{\rm heat}$), which is of magnitude

$$U_{\rm heat} = \int B \, {\rm d}M \rightarrow U_{\rm heat} = \frac{\chi B^2}{2\mu_0(1+\chi)}.$$

Equally, if the applied-field strength is reduced from $H_{C2}(\chi, T)$ to H, the heat ($U_{\rm cool}$) that is in principle absorbed by the paramagnetic ions is

$$U_{\rm cool} = -\frac{\chi B^2}{2\mu_0(1+\chi)} + \frac{1}{2}\mu_0\chi(1+\chi)H_{C2}^2(\chi, T).$$

At this point, we assume that if the applied magnetic field strength is changed, the ions in a paramagnetic superconductor reach thermal equilibrium without absorbing or generating any net heat. Hence the energy that would be transferred to or from the thermal bath is provided by the superelectrons. With this assumption, the magnetic field energy (U_F) is given by

$$U_F = \frac{B^2}{2\mu_0}\frac{1-\chi}{1+\chi} + \frac{1}{2}\mu_0\chi(1+\chi)H_{C2}^2(\chi, T)$$

where $H_{C2}(\chi, T)$ is the applied upper critical field strength necessary to destroy the superconductivity. The equation ensures that the correction which accounts for no net heat transfer to or from the paramagnetic ions to the thermal bath equals zero when the applied field strength H is equal to $H_{C2}(\chi, T)$. At field strengths (H) below $H_{C2}(\chi, T)$, were the material in the normal state, the paramagnetic ions would absorb heat from the thermal bath to reach equilibrium. However, in the superconducting state, this additional energy is provided by the superelectrons. Hence U_F is greater than U_1.

With this expression for U_F, the free energy for a paramagnetic superconductor which accounts for paramagnetic ions is given by

$$F_s(H, T) = F_n(0, T) + \alpha|\psi|^2 + \frac{1}{2}\beta|\psi|^4 + \frac{1}{2m}|(-{\rm i}\hbar\boldsymbol{\nabla} - 2e\boldsymbol{A})\psi|^2 + \frac{B^2}{2\mu_0}\frac{1-\chi}{1+\chi} + \mu_0\chi(1+\chi)\frac{H_{C2}^2(\chi, T)}{2}. \tag{2}$$

With this function, the free energy of the superconducting state and the normal state are equal at $H_{C2}(\chi, T)$, and are obtained from the standard thermodynamic relation

$$F_n(H, T) = F_n(0, T) + (1+\chi)\frac{\mu_0 H^2}{2}. \tag{3}$$

In considering paramagnetic superconductors, the paramagnetic ions are characterized as a medium of susceptibility χ. The distinction between the field produced by the ions ($\mu_0 M_{\rm ions}$), the applied field ($\mu_0 H$) and the field produced by the supercurrents ($\mu_0 M_{sc}$) is now made explicit. In particular, the field produced by the ions is proportional to the local magnetic field produced by the non-paramagnetic-ion sources, so

$$\mu_0 M_{\rm ions} = \chi(\mu_0 H + \mu_0 M_{sc}).$$

This leads to

$$B = \mu_0 H + \mu_0 M_{sc} + \mu_0 M_{\rm ions} = \mu_0(1+\chi)(H + M_{sc}). \tag{4}$$

Using equation (4) to eliminate M_{ions} from equation (2), and minimizing the free energy with respect to $\boldsymbol{A}$ and ψ, keeping H constant, leads to the two Ginzburg–Landau relations, which now include the effect of the paramagnetic ions:

$$\alpha|\psi| + \beta|\psi|^2\psi + \frac{1}{2m}(-\mathrm{i}\bar{h}\boldsymbol{\nabla} - 2e\boldsymbol{A})^2\psi = 0 \tag{5}$$

$$(1+\chi)(1-\chi)\boldsymbol{\nabla} \times \boldsymbol{M}_{sc} = -\frac{\mathrm{i}e\bar{h}}{m}(\psi^*\,\boldsymbol{\nabla}\psi - \psi\,\boldsymbol{\nabla}\psi^*) - \frac{4e^2}{m}\psi^*\psi\boldsymbol{A}. \tag{6}$$

Equations (5) and (6) will be denoted the first and second Ginzburg–Landau equations.

3. Thermal equilibrium in superconductors

In this section we consider how paramagnetic superconductors and normal paramagnetic materials reach thermal equilibrium in a fundamentally different way. Support is provided for the central assumption of this work which is that if the magnetic field applied to a paramagnetic superconductor is changed, after the system has reached thermal equilibrium, there is no net heat generated or absorbed by the paramagnetic ions.

In a normal paramagnetic material, if an applied field is increased, first the splitting between the allowed quantum mechanical states of different magnetic moment increases while the populations of these states remains unchanged. Then, thermal equilibrium is achieved as the populations of these states are rearranged. Moments fall from higher-energy states to lower states, photons are emitted and the material heats up.

Justification for the assumption of no net heat produced or absorbed by the paramagnetic ions (in the superconductor) can be provided by considering the nucleation of a fluxon following an increase in the external field. If the heat that is dissipated in a normal material can be retrieved, then less energy is required to produce the fluxon. If a fluxon is nucleated, a consequence of the phase coherence of the superelectrons is that supercurrents flow to produce flux quantized at ϕ_0. The difference in energy between the allowed states increases for those paramagnetic ions within the fluxon because of the increase in local field. After nucleation, the population numbers of these states will then change as the ions reach thermal equilibrium in the new local field. However, if the magnetic moment of an ion changes (by Δm) by decaying from a higher-energy state to a lower state, additional supercurrent flows to ensure that the total flux remains constant (i.e. ϕ_0). A screening current is produced with a magnetic moment of equal magnitude and opposite sign (i.e. $-\Delta m$). As the paramagnetic ions reach thermal equilibrium, transitions occur for both the paramagnetic ions and the supercurrent which together constitute the fluxon, between quantum mechanical states of the same energy and total flux. The energy that in a normal material would be emitted as photons and dissipated as heat, is *coherently* transferred to the superelectrons to produce the screening currents. We suggest that a general consequence of the phase coherence of the superelectrons is that whenever transitions occur for the paramagnetic ions, screening currents are induced to compensate for the change in the local magnetic field. We conclude that in paramagnetic superconductors, the paramagnetic ions are all in thermal equilibrium with the local field and the thermal bath, but there is no net heat transferred to or from the paramagnetic ions if the external field is changed.

A complete microscopic description of how thermal equilibrium is reached must include a quantum mechanical description of both the magnetic ions and the superelectrons (including surface currents, and the nucleation and motion of fluxons from the surface into the bulk of the material), and include the role of the thermal bath and thermal fluctuations. We have provided support for the assumption of no net heat production,

although a microscopic description is beyond the scope of this work. The remainder of this work considers the implications of this result.

4. High-field calculations

4.1. The upper critical field

Abrikosov [5] was the first to derive an expression for the upper critical field from the Ginzburg–Landau equations. Linearizing the first Ginzburg–Landau equation gives

$$\alpha|\psi_L| + \frac{1}{2m}(-\mathrm{i}\hbar\boldsymbol{\nabla} - 2e\boldsymbol{A})^2\psi_L = 0 \tag{7}$$

where the magnetic vector potential is taken as

$$\boldsymbol{A} = (1+\chi)Hx\boldsymbol{j}.$$

The solution for the wavefunction ψ_L provided by Abrikosov is still valid, where

$$\psi_L(x, y) = \sum_{n=-\infty}^{\infty} C_n \exp(\mathrm{i}nky)\exp\left[-\frac{(x-x_n)^2}{2\xi^2(T)}\right] \tag{8}$$

where C_n are constants, the spacing between the fluxons is $x_{n+1} - x_n$, the upper critical field is $\mu_0\boldsymbol{H}_{C2}(\chi, T)$, and ξ is the coherence length. By substituting the linearized wavefunction ψ_L into equation (7), ξ and H_{C2} are found to be of the form

$$\begin{aligned} \xi^2(T) &= \frac{\hbar^2}{2m|\alpha|} \\ \mu_0 H_{C2}(\chi, T) &= \frac{\phi_0}{2\pi\xi^2(T)(1+\chi)} = \frac{\mu_0 H_{C2}(\chi = 0, T)}{(1+\chi)}. \end{aligned} \tag{9}$$

Equation (9) suggests that the coherence length is unchanged by the presence of the paramagnetic ions. However, the superelectrons experience both the applied field and an additional field produced by the paramagnetic ions. Therefore, the applied field that destroys the superconductivity, the upper critical field ($\mu_0 H_{C2}(\chi, T)$), decreases as χ increases.

4.2. The field dependence of $\boldsymbol{M}$ close to H_{C2}

To determine the field dependence of the total magnetization ($\boldsymbol{M}$), the two Ginzburg–Landau equations must be solved for $|\psi|$ and $\boldsymbol{M}_{SC}$. Just below $\boldsymbol{H}_{C2}$, the wavefunction and the magnetic vector potential can be written [7] as

$$\psi = \psi_L + \psi_1$$

and

$$\boldsymbol{A} = \boldsymbol{A}_{C2} + \boldsymbol{A}_1$$

where $\boldsymbol{A}_1$ and ψ_1 are small, ψ_L is defined by equation (8) and the orthonormality relation is [7]

$$\int (\psi_L^* \psi_1)\ \mathrm{d}^3 r = 0.$$

By definition,

$$\boldsymbol{\nabla} \times \boldsymbol{A}_{C2} = \mu_0(1+\chi)\boldsymbol{H}_{C2}.$$

The expressions for the wavefunction and the magnetic vector potential are substituted into the first Ginzburg–Landau equation and simplified using the orthonormality relation between ψ_1 and ψ_L, and the definition of $\boldsymbol{A}_{C2}$. Then using the second Ginzburg–Landau relation and ignoring surface integrals, and retaining only first-order terms, one finds the result [7]

$$\int (-\boldsymbol{A}_1 \cdot \boldsymbol{\nabla} \times \boldsymbol{M}_{sc} + \beta |\psi_L|^4)\ \mathrm{d}^3 r = 0.$$

Since $\boldsymbol{M}_{sc}$ is orthogonal to $\boldsymbol{A}_1$, this equation can be rearranged using a vector identity and ignoring surface integrals to give [7]

$$\int (-\boldsymbol{M}_{sc} \cdot \boldsymbol{\nabla} \times \boldsymbol{A}_1 + \beta |\psi_L|^4)\ \mathrm{d}^3 r = 0. \tag{10}$$

Abrikosov found that for a wavefunction of the form of equation (8)

$$\frac{e\bar{h}}{m}\left(\frac{\mathrm{d}}{\mathrm{d}x}|\psi_L|^2 - \frac{\mathrm{d}}{\mathrm{d}y}|\psi_L|^2\right) = -\frac{\mathrm{i}e\bar{h}}{m}(\psi_L^* \boldsymbol{\nabla}\psi_L - \psi_L \boldsymbol{\nabla}\psi_L^*) - \frac{4e^2}{m}\psi_L^*\psi_L \boldsymbol{A}.$$

Comparison between this equation and the second Ginzburg–Landau equation gives

$$\boldsymbol{M}_{sc} = \frac{-1}{(1-\chi)(1+\chi)}\frac{e\bar{h}\langle|\psi_L|^2\rangle}{m} \tag{11}$$

where the notation used is

$$\int (|\psi_L|^2)\ \mathrm{d}^3 r = \langle|\psi_L|^2\rangle.$$

The Ginzburg–Landau parameter for a non-magnetic (i.e. $\chi = 0$) superconductor $\kappa(0)$ and the Abrikosov parameter β_A are defined by

$$\begin{aligned} \kappa(0) &= \frac{m^2\beta}{2\mu_0 e^2 \bar{h}^2} \\ \beta_A &= \frac{\langle|\psi_L|^4\rangle}{\langle|\psi_L|^2\rangle^2}. \end{aligned} \tag{12}$$

Substituting the expression for $\boldsymbol{M}_{sc}$ into equation (10) gives the result

$$\int \left(\frac{\mu_0 e\bar{h}|\psi_L|^2}{(1-\chi)m}\left(H - H_{C2}(\chi, T) - \frac{1}{(1+\chi)(1-\chi)}\frac{e\bar{h}|\psi_L|^2}{m}\right) + \frac{2\mu_0\kappa^2(0)e\bar{h}|\psi_L|^4}{m}\right)\mathrm{d}^3 r = 0$$

or equivalently

$$\langle|\psi_L|^2\rangle = -\frac{\mu_0 m}{e\bar{h}}\frac{(1+\chi)(H - H_{C2}(\chi, T))}{(2\kappa^2(0) - 1/(1-\chi))\beta_A}.$$

Substituting this expression into equation (11) gives an expression for the field dependence of the magnetization produced by the superelectrons, of the form

$$\boldsymbol{M}_{sc} = -\frac{\boldsymbol{H}_{C2}(\chi, T) - \boldsymbol{H}}{(2\kappa^2(0)(1-\chi) - 1)\beta_A}. \tag{13}$$

It follows from this equation that if $\chi \ll 1$, M_{sc} is negative as found in standard metallic superconductors. If $\chi \gg 1$, M_{sc} produces a positive contribution to the magnetization below $\mu_0 H_{C2}(T)$. In this paper, the term ferromagnetic (or diamagnetic) superconductivity is used when the effect of the superconductivity is to increase (decrease) the magnetization

above (below) that which would be expected from the paramagnetic ions alone. The term does not necessarily imply that the total magnetization is positive (negative). The change from diamagnetism to ferromagnetism is justified as follows: for $\chi \ll 1$, the response of the paramagnetic superconductor is similar to that of a metallic superconductor. The supercurrent that circulates each fluxon rotates in the same sense as the current that produces the applied magnetic field. When $H = H_{C2}(\chi, T)$, the (screening) supercurrents that flow within the penetration depth of the surface flow in the opposite direction to (and are cancelled by) the net current produced at the surface from the fluxons. As the applied-field strength is reduced, the number of fluxons decreases, and hence the net field produced by the supercurrents opposes the applied field which gives diamagnetism. When $\chi \gg 1$, if a fluxon nucleates, the paramagnetic ions equilibrate by producing a field that is larger than the field produced by the supercurrents that were originally produced at nucleation. Phase coherence (quantization of flux) demands that the supercurrent that rotates around the fluxon produces a negative field—the local net supercurrent rotates in an opposite sense to the current that produces the applied field. Hence as fluxons leave the material, the net supercurrent adds to the applied field which gives ferromagnetism.

Equations (13) and (4) give an expression for the total magnetization $\boldsymbol{M}$ of the form

$$\boldsymbol{M} = \frac{\boldsymbol{B}}{\mu_0} - \boldsymbol{H} = \chi \boldsymbol{H} - \frac{(1+\chi)(\boldsymbol{H}_{C2}(\chi, T) - \boldsymbol{H})}{(2\kappa^2(0)(1-\chi) - 1)\beta_A}. \tag{14}$$

5. The Landau free energy in high magnetic fields

If the expression for the free energy is simplified using the first Ginzburg–Landau equation and surface integrals are ignored, this gives

$$F_s(H, T) = F_n(0, T) - \frac{\beta}{2}|\psi|^4 + \frac{B^2}{2\mu_0}\frac{1-\chi}{1+\chi} + \mu_0(1+\chi)\frac{H_{C2}^2(\chi, T)}{2}. \tag{15}$$

In high fields, $H \approx H_{C2}(T)$, one can take leading terms, and from equations (3) and (13), find

$$F_s(H, T) \approx F_n(H, T) + \frac{\mu_0(1-\chi^2)H(H_{C2}(\chi, T) - H)}{(2\kappa^2(0)(1-\chi) - 1)\beta_A}. \tag{16}$$

For $\chi < 1 - 1/2\kappa^2(0)$ and $\chi > 1 + 1/2\kappa^2(0)$, the free energy in both the diamagnetic and ferromagnetic superconducting state is lower than that in the normal state as required. When $1 - 1/2\kappa^2(0) < \chi < 1 + 1/2\kappa^2(0)$, this is equivalent to the condition that the Ginzburg–Landau parameter ($\kappa(\chi)$) is less than $1/\sqrt{2}$ (i.e. the condition for type I superconductivity in metallic superconductors). The properties of this low-$\kappa(\chi)$ state are discussed in section 7.

6. Low-field calculations

6.1. Flux quantization

The quantization of flux is now considered [8]. The total flux threading a fluxon in the paramagnetic superconductor is produced by two contributions, the circulating supercurrents and the aligned paramagnetic ions. A vortex wavefunction (ψ_V) is used [5, 8], which is a general solution to the Ginzburg–Landau equations of the form

$$\psi_V = \psi_\infty f(r) \mathrm{e}^{\mathrm{i}\phi}$$

where $|\psi_\infty|^2 = -\alpha/\beta$, $f(r)$ is a function of the radius and ϕ is the phase of the wavefunction. One of Maxwell's equations is also used:

$$\boldsymbol{\nabla} \times \boldsymbol{M}_{sc} = \boldsymbol{J}_{sc}. \tag{17}$$

Substituting these two equations into the second Ginzburg–Landau equation gives

$$(1+\chi)(1-\chi)\boldsymbol{J}_{sc} = 2\frac{e\bar{h}N_{sc}}{m} f^2 \boldsymbol{\nabla}\phi - 4e^2 \frac{N_{sc}}{m} f^2 \boldsymbol{A}.$$

Rewriting this equation in terms of a line integral around a closed path gives

$$\int (\boldsymbol{\nabla}\phi)\ \mathrm{d}s = \int \left(\frac{m(1+\chi)(1-\chi)}{2e\bar{h}N_{sc}f^2} \boldsymbol{J}_{sc} \right) \mathrm{d}s - \frac{2e}{\bar{h}} \int \boldsymbol{A}\ \mathrm{d}s.$$

The phase is quantized in units of $2n\pi$. If the path integral is taken so that J_{sc} is zero along the path, then

$$\int \boldsymbol{B} \cdot \mathrm{d}\boldsymbol{S} = \frac{nh}{2e} = n\phi_0$$

and assuming that the paramagnetic ions are in thermal equilibrium, the classic result for non-magnetic superconductors is unchanged, namely that the flux is quantized in units of ϕ_0.

6.2. Magnetic properties in low field, $\chi < 1 - 1/2\kappa^2$

The magnetization in low fields can be calculated from the second Ginzburg–Landau equation. In the Meissner state, there is no flux penetrating the bulk of the superconductor, ψ is constant, $\boldsymbol{\nabla}\psi$ is zero, and

$$(1+\chi)(1-\chi)\boldsymbol{\nabla} \times \boldsymbol{M}_{sc} = -\frac{4e^2}{m}\psi^*\psi \boldsymbol{A}.$$

Taking the curl of both sides and using Maxwell's equation (equation (17)):

$$\mu_0\lambda^2(1+\chi)(1-\chi)\boldsymbol{\nabla} \times \boldsymbol{J}_{sc} = -\boldsymbol{B} \tag{18}$$

where the penetration depth has been introduced, which is defined as

$$\lambda^2 = \frac{m}{\mu_0\, 4e^2\psi^*\psi}. \tag{19}$$

Taking the curl of equation (3) (and using $\boldsymbol{\nabla} \times \boldsymbol{H} = 0$) gives

$$\boldsymbol{\nabla} \times \boldsymbol{B} = \mu_0(1+\chi)\boldsymbol{\nabla} \times \boldsymbol{M}_{sc}.$$

Rewriting the resultant equation using Maxwell's equation and substituting into equation (18), the result is

$$\lambda^2(1-\chi)\boldsymbol{\nabla} \times \boldsymbol{\nabla} \times \boldsymbol{B} + \boldsymbol{B} = 0.$$

Using standard vector manipulation, and Maxwell's equation $\boldsymbol{\nabla} \cdot \boldsymbol{B} = 0$, one finds

$$-\lambda^2(1-\chi)\nabla^2\boldsymbol{B} + \boldsymbol{B} = 0. \tag{20}$$

For $\chi < 1$, equation (20) implies an exponentially decaying solution. This leads to the Meissner state in low fields where the flux is expelled from the bulk of the superconductor.

In the high-$\kappa(0)$ limit, the properties of a fluxon can be described by introducing a delta function of quantized flux [8]. Hence equation (20) is rewritten as

$$-\lambda^2(1-\chi)\nabla^2\boldsymbol{B} + \boldsymbol{B} = \delta(r)\phi_0\boldsymbol{k}.$$

The solutions of this equation which give the field in the vicinity of a fluxon can be written in the form [8]

$$\begin{aligned} B &\to \frac{\phi_0}{2\pi\lambda^2(1-\chi)}\left(\frac{\pi\lambda(1-\chi)^{1/2}}{2r}\right)^{1/2} \mathrm{e}^{-r/(\lambda(1-\chi)^{1/2})} && \text{when } r \to \infty \\ B &\approx \frac{\phi_0}{2\pi\lambda^2(1-\chi)}\left(\ln\frac{\lambda(1-\chi)^{1/2}}{r} + 0.12\right) && \text{where } \xi \ll r \ll \lambda. \end{aligned} \tag{21}$$

The lower critical field ($\mu_0 H_{C1}(\chi, T)$), can be written in terms of ε_1, the energy per unit length of a fluxon, as [8]

$$H_{C1}(\chi, T) = \frac{\varepsilon_1}{\phi_0}.$$

In the high-$\kappa(0)$ limit, ε_1 can be calculated by ignoring the core. Using the expression for the free energy (equation (2)), this gives

$$\varepsilon_1 = \int \mathrm{d}^2 r \left(\frac{1-\chi}{1+\chi}\frac{B^2}{2\mu_0} + \frac{1}{2m}|(-\mathrm{i}\bar{h}\boldsymbol{\nabla} - 2e\boldsymbol{A})\psi|^2\right).$$

Simplifying this equation using the general vortex wavefunction ψ_V, and the second Ginzburg–Landau equation, gives [8]

$$\varepsilon_1 = \frac{1-\chi}{1+\chi}\left[B\ \frac{\mathrm{d}B}{\mathrm{d}r}\ 2\pi r\right]_\xi$$

where the negative value of the bracketed term evaluated at $r = \xi$ is required. Hence using equation (21), the lower critical field is given by

$$\mu_0 H_{C1}(\chi, T) = \frac{1}{(1-\chi)(1+\chi)}\frac{\phi_0}{4\pi\lambda^2}(\ln(\kappa(0)(1-\chi)^{1/2}) + 0.12) \tag{22}$$

which shows that for $\chi < 1 - 1/\kappa^2$, below $\mu_0 H_{C1}(\chi, T)$ one can find a Meissner state region.

6.3. Magnetic properties in low field, $\chi > 1 + 1/2\kappa^2$

A complete description of the low-field properties requires solutions to the non-linear Ginzburg–Landau equations. We assume that in the low-field, high-$\kappa(0)$ limit, one can ignore the cores of fluxons, and the second Ginzburg–Landau equation again leads to equation (20). For $\chi > 1$, equation (20) leads to oscillatory solutions. If it is assumed that the flux is quantized in units of ϕ_0, one of the solutions for equation (20) is of the form

$$B(x, y) = \frac{\phi_0}{8\lambda^2(\chi-1)}\sin\left(\frac{x}{\sqrt{2}\lambda(\chi-1)^{1/2}}\right)\sin\left(\frac{y}{\sqrt{2}\lambda(\chi-1)^{1/2}}\right).$$

More general solutions are required to consider in detail the structure of the flux line lattice. However, this expression is used here to determine the bulk magnetic properties which are not structure sensitive. This solution for $B(x, y)$ suggests that in the low-field region one may find an antiferromagnetic flux structure. We find an approximate expression for the field by which the lattice will have transformed from the low-field antiferromagnetic structure to the high-field ferromagnetic superconducting structure. It is assumed that this low-field approximation breaks down when the internal field that would be produced by the applied field ($\mu_0 H_{M1}(\chi, T)(1+\chi)$) is comparable to the field in the antiferromagnetic structure. This leads to

$$\mu_0 H_{M1}(\chi, T) \approx \frac{\phi_0}{8\lambda^2(\chi-1)(1+\chi)}(\ln(\kappa(0)(\chi-1)^{1/2}) + 0.12) \tag{23}$$

where the factor $\ln(\kappa(0)(\chi - 1)^{1/2}) + 0.12$ has been added, in the light of equation (22) which has been found using a more rigorous calculation. This factor keeps $H_{M1}(\chi, T)$ finite as χ approaches one.

7. The structure of the flux line lattice

7.1. The Ginzburg–Landau parameter

This oscillatory solution and the exponential solution for the magnetic field in low fields suggest that a general expression for the effective penetration depth ($\lambda(\chi)$) is $\lambda|(1-\chi)|^{1/2}$. Similarly, from section 4.1, the effective coherence length ($\xi(\chi)$) is independent of χ. This suggests that the Ginzburg–Landau parameter $\kappa(\chi)$ for a paramagnetic superconductor is given by

$$\kappa^2(\chi) = \frac{\lambda^2(\chi)}{\xi^2(\chi)} = |(1-\chi)|\kappa^2(0). \tag{24}$$

$\kappa(\chi)$ is always greater than zero. In the high-$\kappa(0)$ limit, for very low and very high χ-values, $\kappa(\chi)$ is high, and as χ tends to one, $\kappa(\chi)$ tends to zero.

The expression for the Landau free energy in high fields (equation (16)) suggests that the triangular structure of the flux line lattice is always preferred over the square structure. The minimum value for the free energy always occurs for the triangular lattice for which $\beta_A = 1.16$ [9] rather than the square lattice ($\beta_A = 1.18$) [5]. However, except at fields very close to the upper critical field, the non-linear terms in the Ginzburg–Landau equations must be included and equation (16) is no longer valid. General arguments are provided below to determine the structure of the flux line lattice. These consider the nature of the fluxon–fluxon interactions, through the Ginzburg–Landau parameter $\kappa(\chi)$, and symmetry constraints.

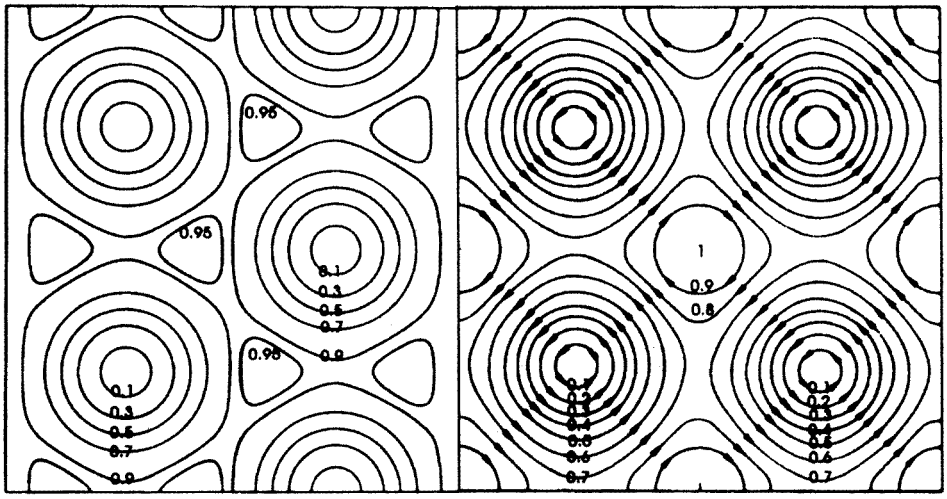

Figure 1. Contour diagrams for $|\psi|^2$ for the triangular lattice of Kleiner *et al* [9] and the square lattice of Abrikosov [5].

7.2. High $\kappa(\chi)$, high magnetic fields

It is very well known that in non-magnetic superconductors when $\kappa(0) > 1$, theoretical calculations [9, 10] and experimental decoration measurements [11] show that the triangular lattice is stable. The preference for the triangular structure, and in particular the relative stability of the triangular lattice compared to the square lattice, can be explained as follows [8]: in the triangular lattice there are six nearest neighbours, and the nearest-neighbour distance is $1.075(\phi_0/B)^{1/2}$. For the square lattice there are only four nearest neighbours, and the nearest-neighbour distance is $(\phi_0/B)^{1/2}$. So for a given flux density, the nearest-neighbour distance for a triangular lattice is greater than that of the square lattice. The dominant interaction between fluxons in non-magnetic superconductors is repulsive, due to the current flow around each fluxon. Hence it is reasonable that the structure with the largest nearest-neighbour separation, namely the triangular lattice, is favoured. Only the stability of the triangular and square lattice need be considered since they are the only structures which tessellate and have the required symmetry such that the location of each fluxon is equivalent. These two structures, which have been described by Abrikosov [5] and Kleiner *et al* [9], are shown in figure 1.

For paramagnetic superconductors, there are two contributions to the forces between the fluxons. There is the repulsive force from the supercurrents that flow around each fluxon. There is also an attractive force of the form $-\boldsymbol{m}_{\text{ions}} \cdot \boldsymbol{B}$ which results from the magnetized magnetic ions being attracted into the higher-field region of neighbouring fluxons.

In the diamagnetic superconducting phase, when $\kappa(\chi) > 1$ which implies the condition $\chi < 1+1/\kappa^2(0)$, the net fluxon–fluxon force is repulsive and a triangular lattice is expected. In the ferromagnetic superconducting phase when $\kappa(\chi) > 1$, $\chi > 1 + 1/\kappa^2(0)$, and fluxons penetrate the bulk of the superconductor. The attractive force between fluxons is larger than the repulsive force and can be explained by considering the general expression for the free energy (equation (2)). For $\chi > 1$, if the fluxon–fluxon spacing decreases, the term $(1-\chi)B^2/2\mu_0(1+\chi)$ decreases, lowering the free energy and implying an attractive force. The general discussion on the structure of the flux line lattice implies that this attractive force between the fluxons will lead to a square flux line lattice.

7.3. High $\kappa(\chi)$, low magnetic fields

It can be seen from equation (22) that in low fields paramagnetic superconductors are in the Meissner state for $\chi < 1 - 1/\kappa^2(0)$. For higher values, $\chi > 1 + 1/\kappa^2(0)$, and $H < H_{M1}$, we have found an antiferromagnetic flux line lattice. In this part of the phase diagram, the dominant force between the fluxons is that between the magnetized paramagnetic ions. Since the field senses in nearest-neighbour fluxons are opposite, the polarities of the magnetized paramagnetic ions are opposite and the force between fluxons is repulsive. This repulsive force will lead to a triangular lattice.

7.4. Intermediate $\kappa(\chi)$-values

For the intermediate κ-values, $1/\sqrt{2} < \kappa < 1$, the coherence length is longer than the penetration depth. Kramer [12] found general non-linear solutions to the Ginzburg–Landau equations which account for the core of the fluxons accurately. In non-magnetic superconductors, over the intermediate range of $\kappa(0)$, when $\mu_0 H > 0.3H_C$, these solutions demonstrate that the force between the fluxons is attractive and the square lattice is stable. The attractive interaction is due to the overlapping cores, and the lower energy of the square lattice compared with the triangular lattice is consistent with the general explanation

provided above. Decoration measurements on Pb–Tl rods [13] show a rectangular lattice, which is consistent with this result.

Using equation (24), the condition for the square lattice to occur, $1/\sqrt{2} < \kappa(\chi) < 1$, is equivalent to $1 - 1/\kappa^2(0) < \chi < 1 - 1/2\kappa^2(0)$ and $1 + 1/2\kappa^2(0) < \chi < 1 + 1/\kappa^2(0)$.

7.5. The low-$\kappa(\chi)$ state

In metallic superconductors, when the Ginzburg–Landau parameter is less than $1/\sqrt{2}$, the material is type I. Throughout the superconducting phase, the material is in the Meissner state. Using equation (24), the condition $\kappa < 1/\sqrt{2}$ implies that $1 - 1/2\kappa^2(0) < \chi < 1 + 1/2\kappa^2(0)$.

At low $\kappa(\chi)$-values, non-linear numerical solutions of the Ginzburg–Landau equations are required to determine accurately the temperature dependence of $\mu_0 H_{C1}(\chi, T)$ and $\mu_0 H_{M1}(\chi, T)$, and the structure of the flux line lattice in these regions. Equation (16) suggests that neither the diamagnetic lattice nor the ferromagnetic lattice is stable in the low-$\kappa(\chi)$ state. For $\chi < 1$, equation (20) suggests that the Meissner state is the lowest energy state and $\mathrm{d}M/\mathrm{d}H$ is -1. For $\chi > 1$, equation (20) suggests that the antiferromagnetic state is found. In this antiferromagnetic state, the cores of the fluxons overlap and in the high-$\kappa(0)$ limit, the structure of the flux line lattice is square.

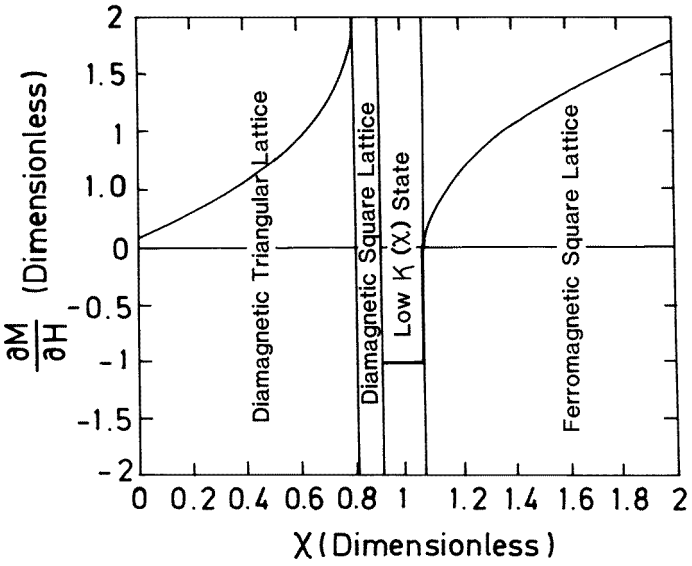

Figure 2. $\mathrm{d}M/\mathrm{d}H$ just below $H_{C2}(\chi, T)$ as a function of the susceptibility, showing the different magnetic phases that occur.

8. Discussion of the results

In figures 2 and 3, graphical representations of the mathematical results found are presented. We have considered a model paramagnetic superconductor where the critical temperature $T_C = 10$ K, and $\mu_0 H_{C2}(\chi = 0, T) = 2.5(1 - T/T_C)$ where $\mu_0 H_{C2}(\chi = 0, T)$ is in tesla. It is assumed that: $\kappa(0) = 2.5$ and is independent of temperature; and $\mu_0 H_{C1}(\chi = 0, T)$

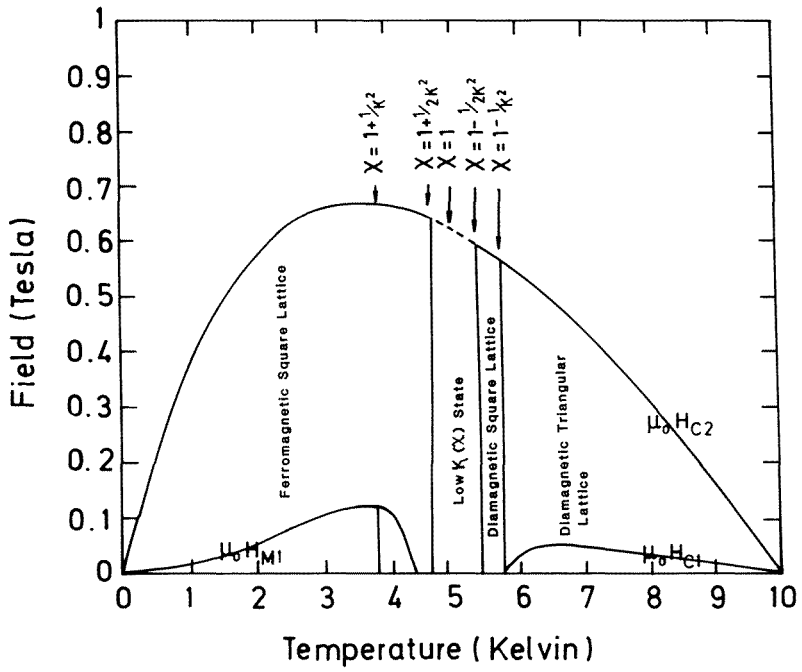

Figure 3. An idealized magnetic phase diagram for a paramagnetic superconductor showing the magnetic phases present in high magnetic fields. The upper critical field is $\mu_0 H_{C2}(\chi, T)$, the lower critical field is $\mu_0 H_{C1}(\chi, T)$, and the field at which the magnetic response changes from ferromagnetic to antiferromagnetic is $\mu_0 H_{M1}(\chi, T)$. In zero field, below $\mu_0 H_{C1}(\chi, T)$, the superconductor is in the Meissner state; below $\mu_0 H_{M1}(\chi, T)$, the magnetic response is antiferromagnetic. In the low-$\kappa(\chi)$ state, $\kappa(\chi) \leqslant 1/\sqrt{2}$.

has the same temperature dependence as $\mu_0 H_{C2}(\chi = 0, T)$. It is also assumed that the susceptibility of the paramagnetic ions in the normal state is described by a simple Curie law of the form $\chi = 5/T$. These values have been chosen for ease of calculation and because they enhance the different regions of the phase diagram that can be found. They also facilitate comparison between the calculations and the experimental data considered in the next section.

In figure 2, the gradient of the magnetization with respect to the applied field ($\mathrm{d}M/\mathrm{d}H$) as a function of χ for the model paramagnetic superconductor is presented. $\mathrm{d}M/\mathrm{d}H$ is given by equation (14) which is valid close to the upper critical field. For low values of χ, there is a diamagnetic triangular flux line lattice and $\mathrm{d}M/\mathrm{d}H$ monotonically increases. For $1-1/\kappa^2(0) < \chi < 1-1/2\kappa^2(0)$, the cores of the fluxons overlap and the diamagnetic lattice has a square structure. In the range $1 - 1/2\kappa^2(0) < \chi < 1 + 1/2\kappa^2(0)$, the low-$\kappa(\chi)$ state is the lowest energy state; for $\chi < 1$, analogously to the case for type I superconductors, the Meissner state is found and $\mathrm{d}M/\mathrm{d}H$ is -1; for $\chi > 1$, equation (20) suggests that the antiferromagnetic state is found. In general the value of $\mathrm{d}M/\mathrm{d}H$ will depend on the orientation of the field with respect to the antiferromagnetic fluxons. The simplest case is taken—it is assumed that the fluxon spacing is independent of the applied field so that $\mathrm{d}B/\mathrm{d}H = 0$ and $\mathrm{d}M/\mathrm{d}H = -1$. There are discontinuities in $\mathrm{d}M/\mathrm{d}H$ at $\chi = 1 \pm 1/2\kappa^2(0)$. For large χ, the gradient increases again, approaching the value of the susceptibility in the

normal state. The structure of the flux line lattice is square and the contribution to the magnetization from the superconductivity is ferromagnetic.

In figure 3, the phase diagram for this model paramagnetic superconductor is described. The upper critical field, $\mu_0 H_{C2}(\chi, T)$, the lower critical field, $\mu_0 H_{C1}(\chi, T)$, and the field for the ferromagnetic/antiferromagnetic phase transition $\mu_0 H_{M1}(\chi, T)$ have been plotted using equations (9), (22) and (23). For high fields, the structure of the flux line lattice and the nature of the contribution to the magnetization from the superconductivity are stated on the figure. In low fields, when $\kappa(\chi)$ tends to zero, complete solutions of the non-linear Ginzburg–Landau equations which fully account for the core of the fluxons will be required to accurately determine the temperature dependence of $\mu_0 H_{C1}(\chi, T)$ and $\mu_0 H_{M1}(\chi, T)$. Below $\mu_0 H_{C1}(\chi, T)$, the material is in the Meissner state. Below $\mu_0 H_{M1}(\chi, T)$, the lattice is antiferromagnetic—triangular structure for $\chi > 1 + 1/\kappa^2(0)$, square structure for $1 < \chi < 1 + 1/\kappa^2(0)$.

Figures 2 and 3 show that in high fields, the contribution to the magnetic response from the superconductivity changes from diamagnetic to ferromagnetic. Hence, if the absence of a diamagnetic superconducting response is taken as evidence for the destruction of superconductivity, then an artifact of this interpretation would be that the upper critical field drops to zero at $\chi = 1$. Equally, one can only expect zero resistance in zero field in the Meissner state. When $\chi > 1$, flux penetrates the bulk of the superconductor, and in high-quality single crystals with low pinning, one can expect a (non-zero) flux flow resistivity [14]. This work suggests that non-zero resistance for $\chi > 1$ cannot be taken as evidence for the destruction of superconductivity. Hence we conclude that the magnetic and resistive response of paramagnetic superconductors when $\chi > 1$ can easily be misinterpreted.

Finally we discuss how the results for the model paramagnetic superconductor may be affected by the inhomogeneities and defects which inevitably occur to some degree in real materials. From figure 2 and equation (14), it is clear that if $\kappa(0)$ is very large, there is only a narrow range of χ over which the low-$\kappa(\chi)$ state will be found. Furthermore if the material is not homogeneous, there will be a distribution in χ. $\mathrm{d}M/\mathrm{d}H$ may never become negative. Rather, as χ increases, $\mathrm{d}M/\mathrm{d}H$ may increase to a peak value at about $\chi = 1$, then decrease, and finally increase again as χ reaches its highest values.

It is well known that in non-magnetic superconductors, it is difficult to measure accurately the properties of the Meissner state. In magnetic measurements, the defects in the material act as flux-pinning sites. Therefore, after the field has been cycled to high values, on returning to zero field there is inevitably flux trapped in the bulk of the superconductor. Hence the magnetic properties are dependent on the history of the magnetic field [15]. One can expect similar history-dependent magnetic properties at high χ-values. If the field has been cycled, on returning to zero field, ferromagnetic domains will be trapped in the bulk of the material and the average magnetic response will be ferromagnetic rather than antiferromagnetic.

9. Comparison with the literature

9.1. Theory

Much theoretical work has been completed on magnetic superconductors. The early work by Matthias *et al* [16] showed competition between magnetism and superconductivity when the superconducting electrons overlap with the localized magnetic moments. Tachiki *et al* [17, 18] have considered the paramagnetic superconductors discussed in this work. It has been shown [19] that Tachiki's results can be described by scaling λ into $\lambda/(1+\chi)^{1/2}$. There is

none of the complexity that we have found at $\chi = 1$. Rather, the superconductor becomes a type I material as χ becomes very large ($\chi > 2\kappa^2(0)$). In particular, ferromagnetism and antiferromagnetism at the lowest temperatures (the highest χ-values) are explained in an entirely *ad hoc* way—for example, by invoking an additional d–f exchange [20]. This is in contrast to this work where the ferromagnetic and antiferromagnetic ordering necessarily occur. The reason for the difference between Tachiki's work and this work originates in the assumption that there is zero heat transfer from the paramagnetic ions as the external field changes in a paramagnetic superconductor.

Below, magnetic, resistive and neutron scattering experimental data found in the literature are considered. Data are presented for the material $ErRh_4B_4$ because of the extensive range of complementary data available. In addition, band-structure calculations show that the conduction electrons are almost completely 4d (Rh) in character with almost no overlap between these electrons and the 4f (Er) electrons in this material [21]. Other paramagnetic superconductors which show similar properties are cited.

9.2. D.C. magnetic properties

In figures 4 and 5, magnetic properties of $ErRh_4B_4$ are shown as functions of field and temperature for the field applied along the a-axis of a single crystal, as given by Behroozi *et al* [22]. The data have been replotted in S.I. units which, on noting the Meissner slope ($\mathrm{d}M/\mathrm{d}H = -1$) in the figures, emphasizes the rapid changes in the properties when the normal-state susceptibility is approximately $+1$.

The gradient in the slope of the magnetization ($\mathrm{d}M/\mathrm{d}H$) at $\mu_0 H_{C2}(T)$ for $ErRh_4B_4$ steadily increases as the temperature drops. Thereafter it reaches a very large peak value at 3 K, and then falls rapidly back to a value equal to the normal-state susceptibility. We explain these results as discussed above using figure 2 and assuming that there is distribution in the values of χ throughout the material. Microscopically this means that when $\chi \approx 1$, in high fields, parts of the material are in the diamagnetic mixed state, and parts in the Meissner state and the superconducting ferromagnetic and antiferromagnetic state. Below 0.7 K, Behroozi *et al* [22] describe the material as being in the normal ferromagnetic state. In the context of this work, the ferromagnetic state is superconducting.

The upper critical field ($\mu_0 H_{C2}(\chi, T)$) of $ErRh_4B_4$ increases from zero at T_C to a maximum value (at about 5.5 K) and thereafter decreases. A similar peak effect has been observed for other rhodium borides, $TmRh_4B_4$ and $HoRh_4B_4$, as well as $DyMo_6S_8$, $HoMo_6S_8$ and $ErMo_6S_8$ [23]. These results are consistent with χ increasing as the temperature decreases and equation (9), as shown in figure 3.

9.3. Resistance measurements

In figure 6, resistance measurements made by Maple *et al* (see [23, 24]) in a nominally zero D.C. magnetic field for $ErRh_4B_4$ are shown. The resistance drops to zero between about 8.5 K and 1 K. Below 1 K, the resistance increases but not to the value found above 8.5 K. This low, non-zero resistance found at the lowest temperatures is consistent with flux penetration and resistive flux flow. Measurements on $HoMo_6S_8$ show a similar reduction in resistance at the lowest temperatures to about 70% of the normal-state resistance above T_C. Furthermore, in this material, measurements have shown that the resistance is dependent on the history of the magnetic field. In the ferromagnetic state, at 25 mK, if the field is applied in one direction and then reversed, the zero-resistance state is reinstated [23, 25]. This history-dependent resistance can be interpreted as evidence for flux pinning and hence

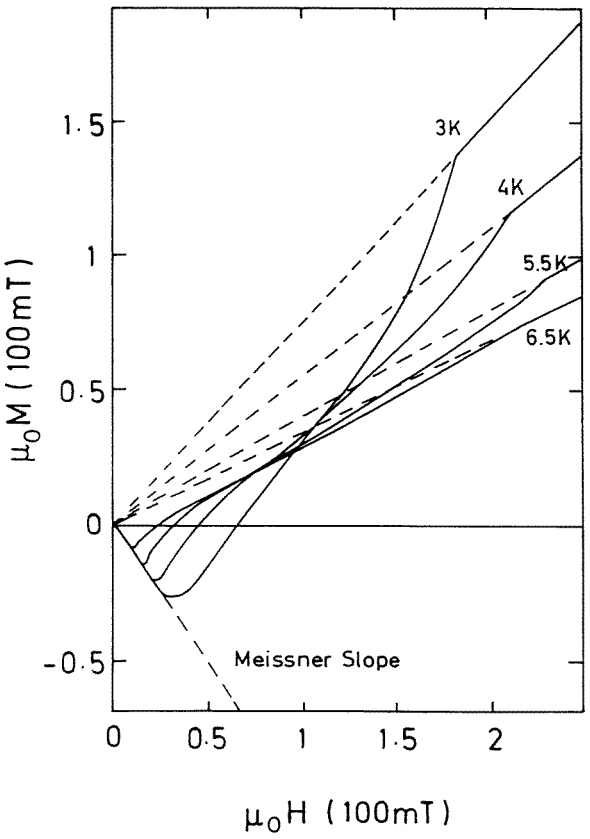

Figure 4. Virgin magnetization curves versus the applied field along the *a*-axis of a single crystal of $ErRh_4B_4$ for $T \geqslant 3$ K taken from reference [22].

is consistent with the origin of the ferromagnetism being superconductivity.

It is noted that if the resistance is zero over a discrete range of temperature or field in a *B–T* phase diagram, it is often taken as evidence for re-entrant superconductivity or field-induced superconductivity [26]. This work suggests that non-zero resistance in zero field does not imply the destruction of superconductivity. In paramagnetic superconductors, below T_C, in the ferromagnetic and antiferromagnetic state, the material remains a bulk superconductor.

9.4. Neutron measurements

Small-angle neutron measurements on $ErRh_4B_4$ have confirmed the ferromagnetic state at the lowest temperatures [27, 28]. Measurements on Chevrel-phase superconductors provide evidence for the coexistence of magnetic order and superconductivity [29, 30]. Recently Yaron *et al* have completed very detailed small-angle neutron scattering investigations on the material $ErNi_2B_2C$ [3]. These results demonstrate that there is the microscopic coexistence of magnetism and superconductivity. Significantly, they find that the lattice is a square lattice over the whole range of the experiment: $0.2\ \text{T} < \mu_0 H < 1.2\ \text{T}$; $1.6\ \text{K} < T < 8.0\ \text{K}$. Yaron *et al* note that the origin of the square lattice is an open question, but speculate that magneto-elastic coupling is one of very few explanations to date

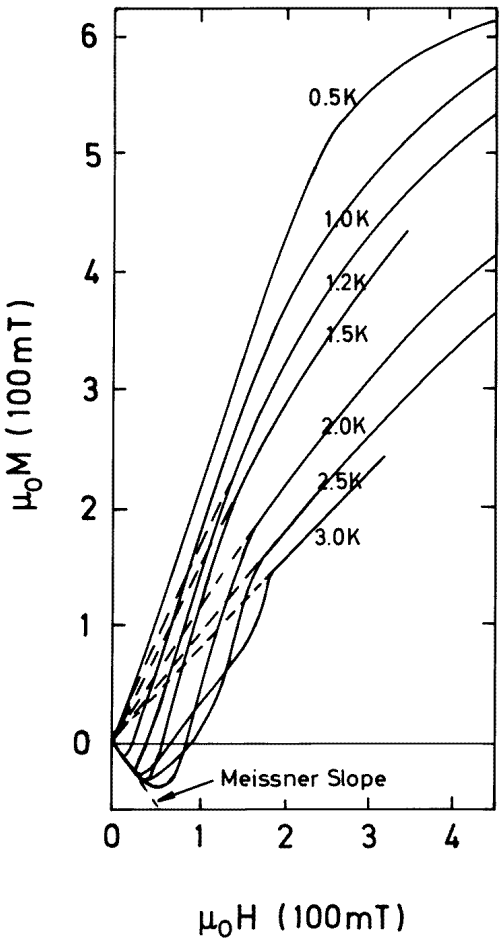

Figure 5. Virgin magnetization curves versus the applied field along the a-axis of a single crystal of $ErRh_4B_4$ for $T \leqslant 3$ K taken from reference [22].

[31]. A complete understanding of Yaron's results will require analysis of the anisotropic properties of $ErNi_2B_2C$. Nevertheless, in the context of this work, the simple explanation for the square lattice is that the susceptibility is greater than $1 - 1/\kappa^2(0)$.

10. Magnetic materials

The special class of paramagnetic superconductors considered in this work is a subset of magnetic superconductors. However, one can expect the range of properties described in this work, notably at $\chi \approx 1$, to occur in many superconducting systems which incorporate strongly paramagnetic ions. Typical values of the susceptibility for materials containing rare-earth ions can be calculated using the Langevin function. Taking a typical unit-cell size for magnetic superconductors of say $\sim$5 Å, at a temperature of 1 K we find $\chi \approx 0.06 p_{\mathrm{eff}}^2$ where p_{eff} is the effective Bohr magneton number. The rare-earth elements have p_{eff}-values up to $\sim 10\mu_B$ which gives $\chi \approx 6$, so values of $\chi \approx 1$ are to be expected.

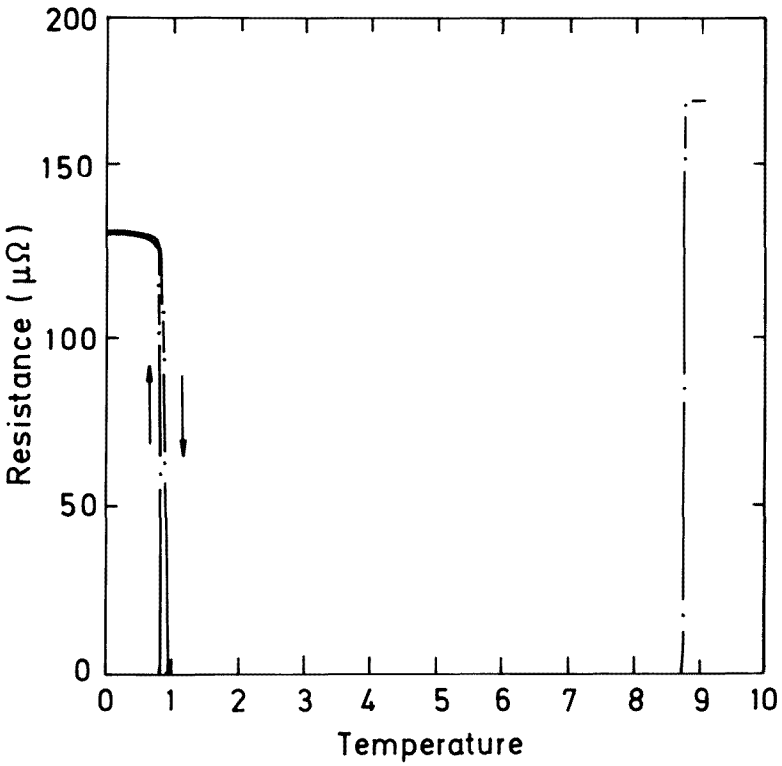

Figure 6. The A.C. electrical resistance versus temperature for $ErRh_4B_4$ taken from reference [23].

A range of magnetic materials provide some further support for the implicit generalization of this work, namely that paramagnetic superconductors with high susceptibility will tend to produce a ferromagnetic or antiferromagnetic resistive superconducting state. The rhodium–boride superconductors with strongly paramagnetic ions, $DyRh_4B_4$, $TbRh_4B_4$ and $GdRh_4B_4$, show a distinct drop in resistance to a non-zero value and ferromagnetic ordering at low temperatures [23, 32]. In the nickel boride carbides, the materials with strongly paramagnetic ions, $DyNi_2B_2C$ and $TbNi_2B_2C$, show a distinct drop in resistance to a non-zero value, whereas those nickel borides with weakly paramagnetic ions containing Y, Lu and Tm show a drop in resistance to a zero value [33]. In the Heusler-type compounds $(RE)Pd_2Sn$ [23, 34], zero resistance is observed in those materials containing weakly paramagnetic ions Y, Tm, Yb, and Lu, whereas antiferromagnetic ordering is found at the lowest temperatures when the ion is strongly paramagnetic—Gd, Tb, Dy, and Ho.

In this work, it has been assumed that the magnetic ions are simply paramagnetic and isotropic. The Ginzburg–Landau equations considered in this work will need to be developed further to explain the two-dimensional and layered high-temperature superconductors. As a more complete picture of the properties of the vast range of magnetic superconductors is developed (including those quoted in this section), one can be sure that in addition to the electromagnetic interaction considered in this work, other interactions must be added for a complete description of these materials.

11. Final comments

A new expression for the Landau free energy of paramagnetic superconductors is presented in this paper. It is based on the assumption that in the superconducting state, if the applied magnetic field is changed, there is no net heat generated or absorbed by the paramagnetic ions after equilibrium has been reached. This provides a framework which can describe much of the data on these materials. In particular it is expected that paramagnetic superconductors with strongly paramagnetic ions will often produce a square flux line lattice structure.

Acknowledgments

The author thanks A Hampshire for her support during this work.

References

[1] Matsubara T and Kotani A (ed) 1984 *Superconductivity in Magnetic and Exotic Materials* (Berlin: Springer)
[2] Fischer O and Maple M B (ed) 1982 *Superconductivity in Ternary Compounds* (Berlin: Springer)
[3] Yaron U, Gammel P L, Ramirez A P, Huse D A, Bishop D J, Goldman A I, Stassis C, Canfield P C, Mortensen K and Eskildsen M R 1996 *Nature* **382** 236
[4] Abrikosov A A and Gorkov L P 1961 *Sov. Phys.–JETP* **12** 1243
[5] Abrikosov A A 1957 *Sov. Phys.–JETP* **5** 1174
[6] Ginzburg V L and Landau L D 1950 *Sov. Phys.–JETP* **20** 1064
[7] Tilley D R and Tilley J (ed) 1990 *Superfluidity and Superconductivity* (Bristol: Hilger)
[8] Tinkham M 1996 *Introduction to Superconductivity* (New York: McGraw-Hill)
Parks R D 1969 *Superconductivity* (New York: Decker)
[9] Kleiner W H, Roth L M and Autler S H 1964 *Phys. Rev.* **133** 1226
[10] Matricon 1964 *J. Physique Lett.* **9** 289
[11] Essmann U and Trauble H 1966 *Phys. Lett.* **24A** 526
[12] Kramer L 1966 *Phys. Lett.* **23** 619
[13] Obst B 1969 *Phys. Lett.* **28A** 662
[14] Kim Y B, Hempstead C F and Strnad C R 1965 *Phys. Rev.* **139** A1163
[15] Kupfer H and Wolfgang K 1977 *Phil. Mag.* **36** 859
[16] Matthias B T, Suhl H and Corenzwit E 1958 *Phys. Rev. Lett.* **1** 92
[17] Tachiki M, Matsumoto H and Umezawa H 1979 *Phys. Rev.* B **20** 1915
[18] Matsumoto H, Umezawa H and Tachiki M 1982 *Phys. Rev.* B **25** 6633
[19] Gray K E 1983 *Phys. Rev.* B **27** 4157
[20] Fischer O, Treuvaud A, Chevrel R and Sergent M 1975 *Solid State Commun.* **17** 721
[21] Freeman A J and Jarlborg T 1982 *Superconductivity in Ternary Compounds* ed O Fischer and M B Maple (Berlin: Springer)
[22] Behroozi F, Crabtree G W, Campbell S A and Hinks D G 1983 *Phys. Rev.* B **27** 6849
[23] Fischer O 1990 *Ferromagnetic Materials* vol, ed K H J Buschow and E P Wohlfarth (Amsterdam: Elsevier Science) p 466
[24] Maple M B, Hamaker H C, Woolf L D, MacKay H B, Fisk Z, Odoni W and Ott H R 1980 *Crystalline Electric Field and Structural Effects in f-Electron Systems* ed J E Crow, R P Guertin and T W Mihalisin (New York: Plenum)
[25] Giroud M, Genicon J L, Tournier R, Geantet C, Pena O, Horyn R and Sergent M 1987 *Physica* B **148** 113
[26] Jaccarino V and Peter M 1962 *Phys. Rev. Lett.* **9** 290
[27] Moncton D E, McWhan D B, Schmidt H, Shirane G, Thomlinson W, Maple M B, MacKay H B, Woolf L D, Fisk Z and Johnston D C 1980 *Phys. Rev. Lett.* **45** 2060
[28] Sinha S K, Crabtree G W, Hinks D G and Mook H 1982 *Phys. Rev. Lett.* **48** 950
[29] Thomlinson W, Shirane G, Moncton D E, Ishikawa M and Fischer O 1981 *Phys. Rev.* B **23** 4455
[30] Burlet P, Dinia A, Quezel S, Erkelens W A C, Rossat-Mignod J, Horyn R, Pena O, Geantet C, Sergent M and Genicon J L 1987 *Physica* B **148** 99
[31] Ullmaier H, Zeller R and Dederichs P H 1973 *Phys. Lett.* **44A** 331

[32] Matthias B T, Corenzwit E, Vandenberg J M and Barz H 1977 *Proc. Natl. Acad. Sci. USA* **74** 1334
[33] Eisaki H, Takagi H, Cava R J, Batlogg B, Krajewski J, Peck W F Jr, Mizuhashi K, Lee J O and Uchida S 1994 *Phys. Rev.* B **50** 647
[34] Ishikawa M, Jorda J L and Junod A 1981 *Proc. Int. Conf. on Superconductivity in d- and f-band Metals* ed W Buckel and W Weber (Karlsruhe: Kernforschungszentrum) p 141